Supplemental methods

Materials

BV421-labelled anti-human CD63 monoclonal antibody (mAb), BV510-labelled anti-human CD42a mAb, BV510-labelled anti-human CD42b mAb, FITC-labelled anti-human CD61 mAb, FITC-labelled PAC1 mAb, PerCP-Cy5.5-labelled anti-human CD36 mAb, PE mouse anti-human platelet GPVI antibody, PE-Cy5 mouse anti-human CD62P antibody and Cytofix were purchased from BD Biosciences (Franklin Lakes, NJ, USA). PE-labelled anti-human GPVI mAb was obtained from BioCytex (Marseille, France). AlexaFluor488- and APC-labelled anti-HLA-A,B,C monoclonal antibodies and mouse-anti CD235a antibody were from BioLegend (San Diego, CA, USA). AKT1+2+3-$^{pY315+316+312}$-AF488 was obtained from Bioss Antibodies (Woburn, MA, USA). CD45-dynabeads and M280 sheep-anti-mouse IgG-dynabeads were from ThermoFisher (Waltham, MA, USA). Fluo-4-AM was obtained from ThermoFisher (Waltham, MA, USA). Aspirin was obtained from Sigma Aldrich (Darmstadt, Germany).

Cross-linked collagen-related peptide (CRP-XL) was obtained from CambCol Laboratories (Cambridge, UK). 2-Methylthioadenosine-diphosphate (2-MeSADP; stable ADP analogue) and D-phenylalanyl-L-prolyl-L-arginine chloromethylketone (PPACK) were from Santa Cruz Biotechnology (Dallas, TX, USA) and thrombin receptor activating peptide 6 (TRAP6) from Bachem (Bubendorf, Switzerland). Triton-X was from Carl Roth (Karlsruhe, Germany). Oligo-dA/dT were from Eurogentec (Seraing, Belgium). Collagen (Horm) was from Nycomed (Zurich, Switzerland). PerFix-nc kit was from Beckman Coulter (Brea, CA, USA). Apyrase was obtained from Merck (Darmstadt, Germany). Acid citrate dextrose solution A was from Fresenius (Bad Homburg vor der Höhe, Germany). Bovine serum albumin (BSA) was obtained from

Serva (Heidelberg, Germany). Glucose was from B.Braun (Melsungen, Germany). Quick-RNA MiniPrep kit was from Zymo Research (Freiburg, Germany).

Platelet preparations

Preparation of the unsorted, large and small platelet fractions

3 mL PRP was centrifuged (650 x g for 7min). The pellet contained the large platelet fraction and the supernatant the small platelet fraction. The latter was aliquoted in 1mL portions and spun down (650 x g, 7 min, RT) to receive a pellet with small platelets. All pellets were resuspended in Tyrode's buffer containing 0.35 % BSA and 0.1 % glucose. Cell counts were adjusted to 300.000/µL. The separation resulted in large platelets with an MPV of 11.1 ±1.3 fL and small platelets with an MPV of 6.9 ± 0.7 fL.

Whole blood perfusion experiments

Samples were recalcified (7.5 mM $CaCl_2$, 3.75 mM $MgCl_2$ in HEPES buffer) in presence of a thrombin inhibitor (40 µM PPACK). Blood was then supplemented with $DiOC_6$ (0.5 µg/mL) and perfused through a transparent parallel-plate perfusion chamber, containing a coverslip coated with collagen type I (100 µg/mL, HORM, Takeda, Hoofddorp, The Netherlands). Perfusion was performed for 4 minutes at a wall-shear rate of 1,000 s^{-1} and kinetics were determined by capturing brightfield and $DiOC_6$ images every 30 seconds at one spot. Thereafter, platelet activation properties were determined by post-staining for P-selectin expression using AF647-conjugated anti-CD62P mAb (1:80, BioLegend, San Diego, CA, USA). Post-perfusion brightfield and fluorescence images were randomly captured throughout the microspot. All images were captured using an EVOS-FL microscope (Life Technologies, Carlsbad, CA, USA) and an Olympus UPLSAPO 60x oil-immersion objective and analysed using specific (half-automated) scripts in the open-access Fiji software (Laboratory for Optical and

Computational Instrumentation, University of Wisconsin-Madison, Madison, WI, USA) as described before [1]. The multilayer size was obtained from brightfield images using a specific (half-automated) script in Fiji software to obtain a percentage surface area coverage for visually present multilayers of platelets. The image analysis, scoring and methods have been described in detail [2,3].

For comparative data analysis, heatmaps were generated from the mean values per parameter. Data was scaled to a range from 0 to 10 based on the highest value of each parameter. To clearly visualise the effects, a subtraction heatmap was created by subtracting the scaled control data from each condition. Heatmaps were generated using R Core Team (i386 3.2.5, Vienna, Austria).

Clustering analysis of multicolour flow cytometry data

Separate FCS files were opened in FlowJo V10 software (Ashland, OR, USA) and checked for data anomalies by FlowAI [4]. The samples were gated for single cells and the presence of CD42a or CD42b, depending on the antibody combination used. The event count per sample was set at 5,000 events using DownSample for equal weighing of each sample before concatenation. The resulting file was subjected to FlowSOM analysis to search for clusters [5]. FlowSOM analysis of platelets is done as described previously [6]. The original sample conditions were retrieved by gating on the SampleID parameter in the concatenated file and the percentages of platelets present in the resulting FlowSOM populations were determined. Characterisation of the resulting populations was done by the markers' expression levels; -/+ indicates within ±1 SD from the mean population mean fluorescence intensity (MFI), --/++ indicates within ±2 SD from the mean population MFI. To visualise these high-dimensional multicolour flow cytometric data in a two-dimensional plot, t-distributed stochastic neighbour embedding (tSNE) analysis was applied.

Conventional flow cytometry

Platelet activation of GPVI-rich platelets

Unseparated, large and small platelets were double stained with PE-labelled anti-human GPVI mAb (1:100) together with either FITC-conjugated PAC1 mAb (1:20), BV421-conjugated CD63 mAb (1:100), or PE-Cy5 mouse anti-human CD62P antibody (1:10), whilst being stimulated with CRP-XL (5 µg/mL), 2-MeSADP (5 µM) or TRAP6 (25 µM) for 15 minutes. The PAC1- and CD63-stained measurements were performed on a BD FACSCanto II, whereas the CD62P-stained measurements were carried out on a Cytoflex flow cytometer. The top 25% GPVI-expressing (GPVI-rich) were gated as described (Figure S1B).

RNA quantification

The RNA-content was determined using a double stain procedure for RNA to exclude the influence of unspecific binding [7]. Platelets were fixed with 0.5% paraformaldehyde for 20 min, centrifuged (650 x g, 7min), permeabilised with 0.1% Triton-X for 10 min and spun down at 650 x g, 7min. The resulting pellet was stained with either oligo-dA-Cy5 (does not bind mRNA), or oligo-dT Cy5 (specific for mRNA) in darkness for 1h. The proportion of RNA-positive platelets was determined as difference between oligo-dT Cy5 and oligo-dA-Cy5 positive events.

HLA- and GPVI- quantification on reticulated platelets

Comparison of HLA or GPVI-expression on reticulated or non-reticulated platelets was performed using double staining. Platelets were first stained with PE-conjugated anti-HLA-A,B,C-antibody or PE-conjugated mouse anti-human platelet GPVI antibody for

20 min at RT in dark. Afterwards, the platelets were fixed and stained using the oligo-dA/dT staining for identification of platelet age as described above. GPVI and HLA levels were quantified on reticulated and non-reticulated platelets using a Cytomics FC500 flow cytometer (Beckman Coulter, Brea, CA, USA).

Signal transduction

Large and small platelets (300.000 cells/µl) were incubated with collagen (5 µg/mL final concentration) for 30-600 sec. Activated cells were fixed and permeabilised using the PerFix-nc kit according to the manufacturer´s instructions. Staining with AKT1+2+3-$^{pY315+316+312}$-AF488 (1:200 final) was performed simultaneously with the permeabilisation step. Afterwards, the platelets were measured using a Cytoflex flow cytometer (Beckman Coulter) and the cells positively gated for AKT1+2+3-$^{pY315+316+312}$-AF488 were quantified compared to unstimulated samples.

To determine signal transduction in reticulated cells, unseparated platelets were stimulated with collagen (5 µg/mL final) for 30-600 sec and fixed, permeabilised and stained as described above. After staining with AKT1+2+3-$^{pY315+316+312}$-AF488, the RNA-content was determined using the oligo-dA/dT method as described above and the cells were measured using a Cytoflex flow cytometer.

Flow cytometric measurements in platelets of ITP patients

RNA-rich platelets were identified using the oligo-dA/dT method, as described above. These platelets were co-stained with either AlexaFluor488-labelled HLA-A,B,C mAb or PE-conjugated GPVI mAb and measurements were performed on BD Accuri C6 cytometer (BD Bioscience, Franklin Lakes, NJ, USA). Platelet activation was determined by staining with FITC-conjugated PAC1 mAb (1:20), BV421-conjugated CD63 mAb (1:100) together with PE-labelled anti-human GPVI mAb (1:100), whilst

being activated by CRP-XL (5 µg/ml), TRAP6 (25 µM) or 2-MeSADP (5 µM). These measurements were done using a Cytek Aurora flow cytometer (Cytek Biosciences, Fremont, CA, USA). Gating for the GPVI-rich platelets was done as described (Figure S1B).

Platelet activation in aspirin-treated large and small platelets

To analyse the effect of secreted thromboxane on the function of large and small platelets, large and small platelets (aspirin pre-treated or untreated) were incubated with 20µM TRAP-6 or 5 µg/mL CRP-XL for 10 min at 37°C. Cells were stained with PE-Cy5 mouse anti-human CD62P antibody (1:10) and measurements were carried out using a FC500 flow cytometer (Beckman Coulter, Brea, CA, USA).

Quantification of HLA and GPVI on RNA-rich and RNA-poor platelets using 15 FSC gates

To exclude platelet size related bias in the quantification of HLA and GPVI on RNA+ and RNA- platelets, we split unseparated platelets into consecutive 15 FSC gates to allow comparison of similar size platelets only. Platelets were first stained with PE-conjugated HLA-A, B, C-antibody or PE-conjugated mouse anti-human platelet GPVI antibody for 20 min at RT in dark. Afterwards, the platelets were fixed and stained using the oligo-dA/dT staining for identification of platelet age as described in the main methods section and GPVI and HLA levels were quantified on reticulated and non-reticulated platelets in each gate using a Cytomics FC500 (GPVI) or a Cytoflex S (HLA) flow cytometer (Fig. S1).

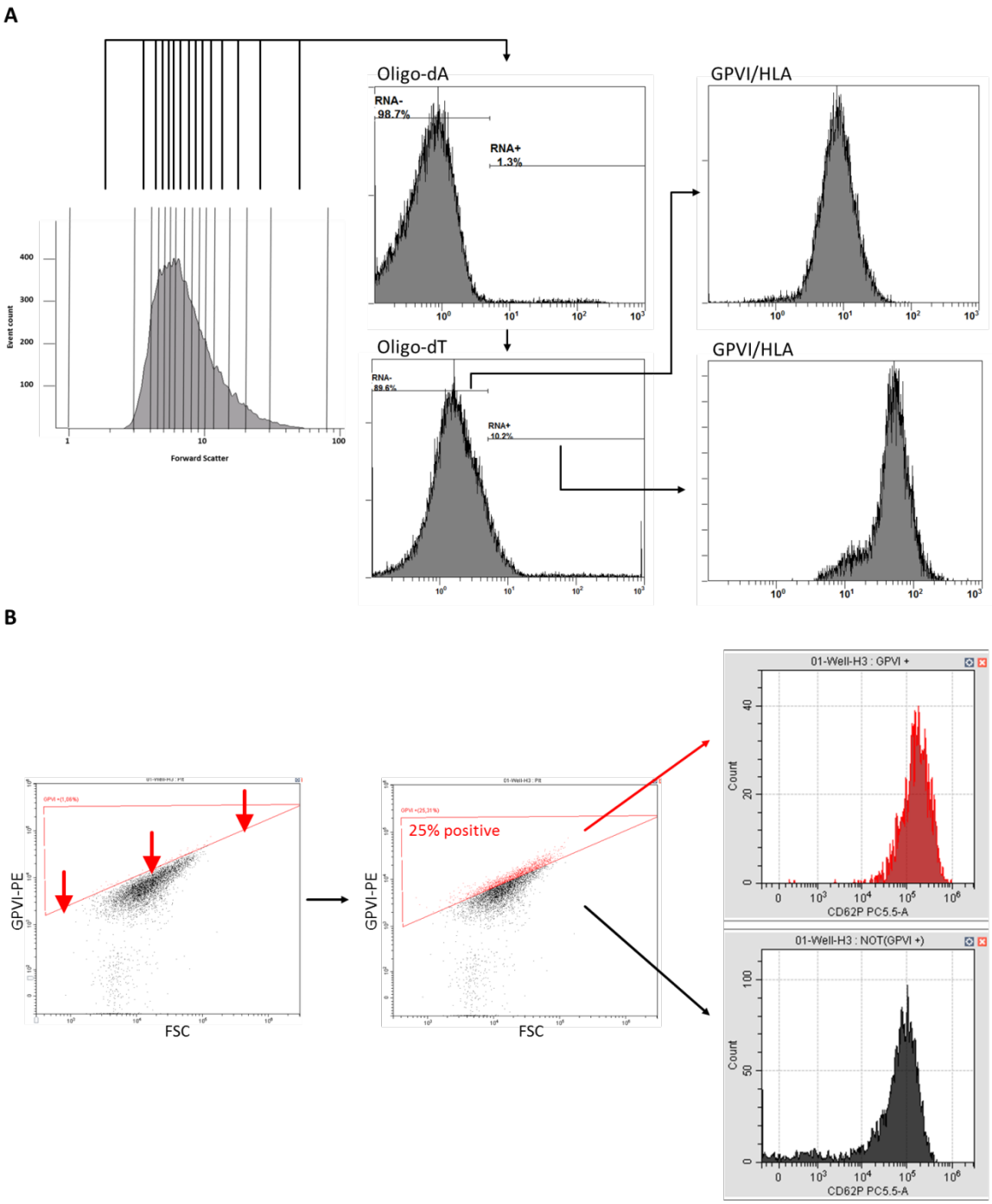

Figure S1: Gating strategy

(A) To quantify GPVI and HLA-1 on RNA+ and RNA- platelets, unseparated platelets were split into 15 consecutive forward scatter gates. RNA+ and RNA- platelets were identified using the Oligo-dA/dT staining method. GPVI or HLA was determined for RNA RNA+ and RNA- platelets in each forward scatter gate separately; (B) To assess CD62P expression of GPVI-rich and GPVI-poor platelets, unseparated platelets were stimulated with TRAP6 or CRP-XL. To avoid a platelet size related bias, the highest GPVI expressing platelets were gated over the complete Forward scatter distribution and CD62P expression was determined in the resulting populations.

Supplemental data

Individual profiles of platelet populations found by clustering analysis

To address and visualize interindividual variability of the platelet subpopulations, we provide a subtracting heatmap (subtracting the scaled large platelet data from the unsorted or small data – Figure S2).

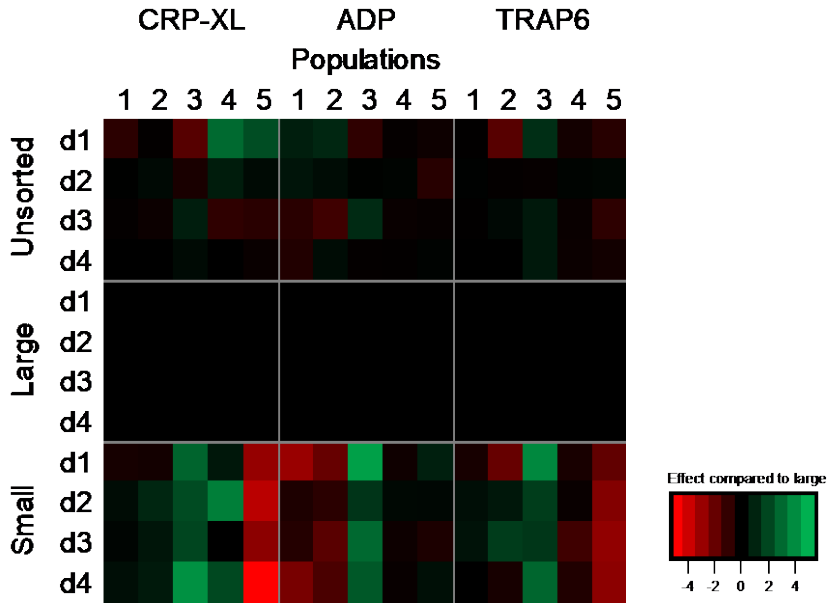

Figure S2: Individual profiles of platelet populations in Figure 2. The data was scaled to a range from 0 to 10 based on the highest value for each population. To clearly visualise the effects between large and small platelets per donor, a subtraction heatmap was created by subtracting the scaled large platelet data from the unsorted or small data per donor.

RNA+ platelets express more HLA and GPVI

The proportions of RNA-positive and RNA-negative platelets were analysed for unseparated platelets in 15 consecutive forward scatter gates as described in the supplemental methods section. We found that with increasing cell size, the proportion

of RNA-positive platelets increased from 5.1% (±5.7) in the gate with the smallest platelets to 73.4% (±35.7) in the gate with the largest platelets (Fig. S3A).

Next, we quantified HLA-I surface expression on RNA-positive and RNA-negative platelets. Here, HLA-I-expression was significantly higher on RNA positive compared to RNA negative cells in all 15 consecutive forward scatter gates. Again, we found the highest HLA-I expression in RNA-positive large platelets (Fig. S3B).

Similar results were obtained when measuring GPVI expression on RNA-positive and RNA-negative platelets. RNA positive platelets expressed significantly more GPVI compared to their RNA negative counterparts in all forward scatter gates (Fig. S3C), a pattern which was again strongest in the FSC-gate for the largest platelets.

These data show that also while comparing cells of similar size in the single gates, RNA+ platelets express more HLA and GPVI on their surface. Therefore, we can exclude a size related artefact in these measurements.

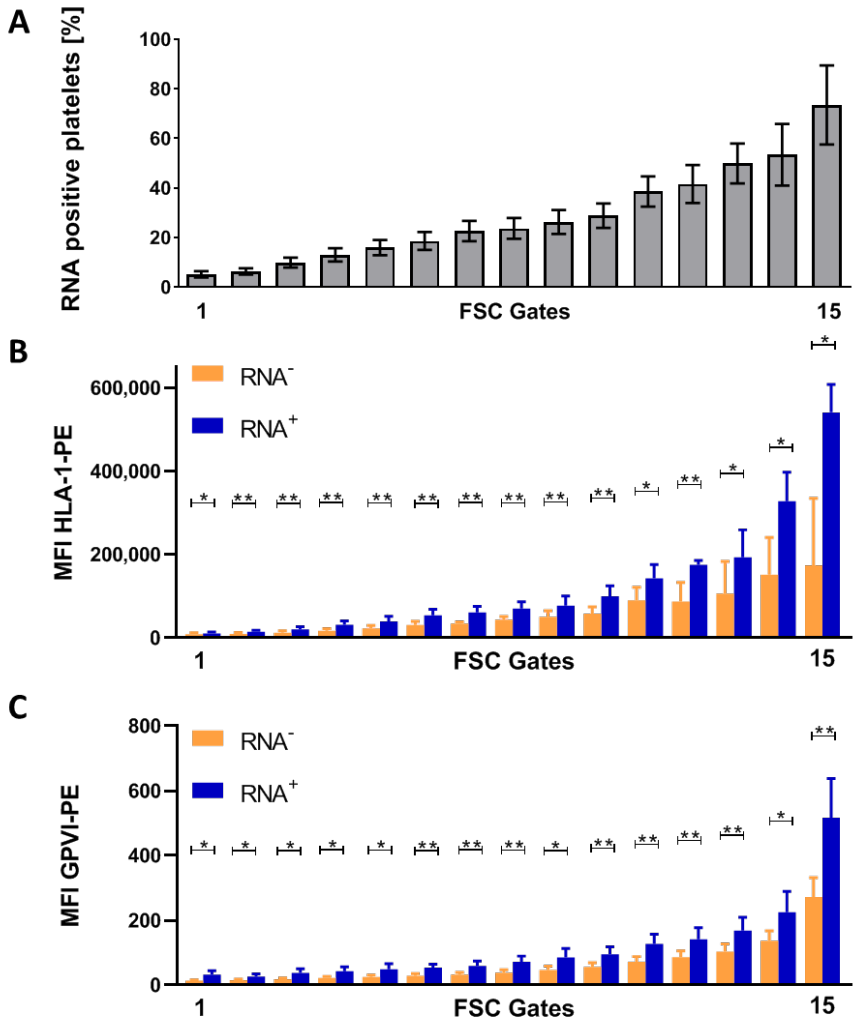

Figure S3: Correlation of platelet size, RNA-positive platelets, HLA-I, and GPVI. (A) The proportion of RNA-positive platelets was determined by T-oligonucleotides in unseparated platelets in 15 consecutive forward scatter gates. Correlation of RNA-positive platelets and (B) HLA-1 expression or (C) GPVI expression was determined by co-staining using T-oligonucleotides and HLA-A,B,C-antibody or GPVI-antibody in unseparated platelets in 15 consecutive forward scatter gates; Mean (+SEM), $n \geq 4$, * $p<0.05$, ** $p<0.01$.

Aspirin treatment does not alter the functional differences between large and small platelets

To determine whether thromboxane released from large and small platelets impacts their function, we incubated ACD-A anticoagulated whole blood with 10 µg/ml (final) of aspirin for 30 min at RT. Afterwards, large and small platelets were prepared as described in the main article and the supplemental methods section.

Afterwards, we analyzed their mobilisation of Ca^{2+} from internal stores to the cytoplasm and their activation after stimulation with 20µM TRAP-6 or 5 µg/mL CRP-XL.

The Ca^{2+}-release assay was performed by fluorescent labelling of free intracellular Ca^{2+}. Platelets were resuspended in Tyrode buffer without $MgCl_2$ and $CaCl_2$ (pH 7·2), adjusted to 150,000/µL and stained with Fluo-4-AM as described (Handtke 2020, Ca paper). Measurements were carried out in a Fluoroskan Ascent FL fluorometer (ThermoFisher, USA). Free intracellular Ca^{2+} was measured in resting platelets and after addition of 20µM TRAP-6 or 5 µg/mL CRP-XL. P-selectin expression was determined using flow cytometry as described in the supplemental methods section.

Large platelets mobilised more Ca^{2+} from their intracellular stores after stimulation with TRAP6 or CRP-XL (Figure S4). Ca^{2+} mobilisation was slightly reduced for both, large and small aspirinated platelets compared to their untreated counterparts after stimulation with TRAP6 or CRP-XL, but the stronger Ca^{2+} mobilisation seen in large platelets remained.

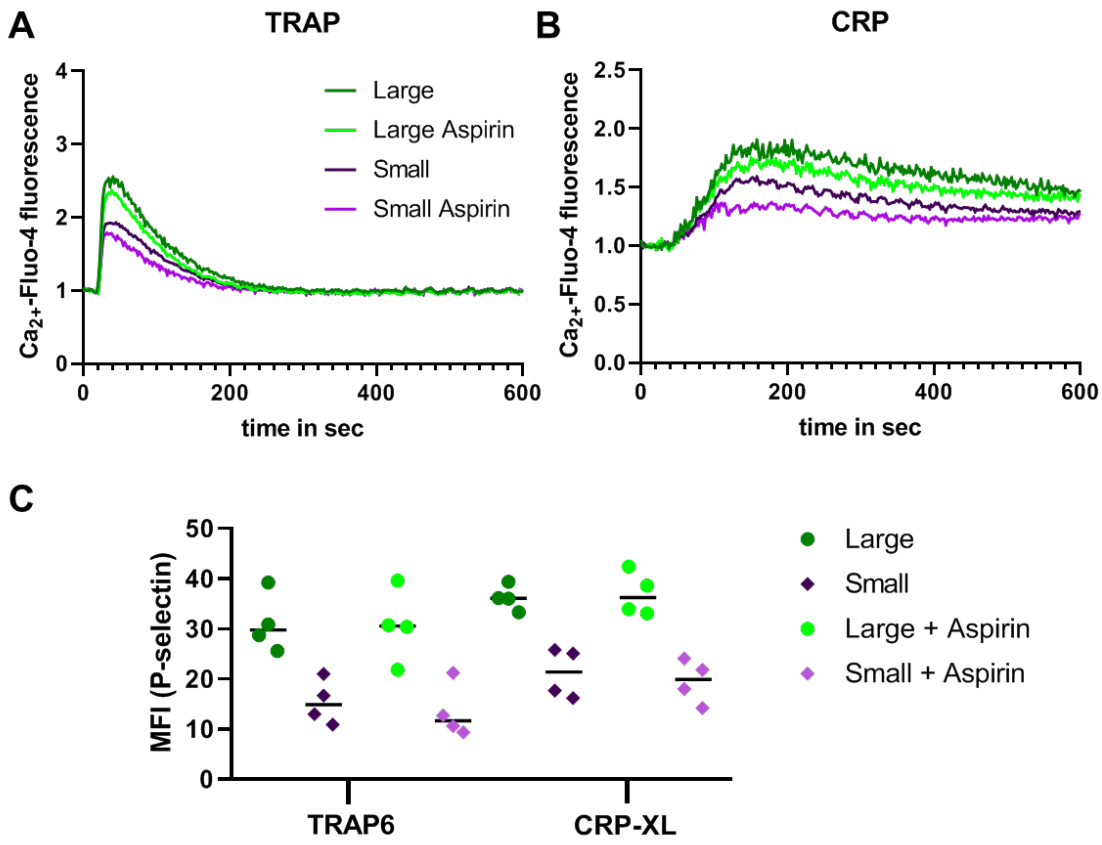

Figure S4: Ca^{2+} mobilisation and activation of aspirin treated large and small platelets. Mobilisation of intracellular Ca^{2+} of large and small platelets with or without aspirin treatment after stimulation with (A) TRAP6 (20 µM) and (B) CRP-XL (5 µg/ml); (C) P-selectin expression of large and small platelets with or without aspirin treatment after stimulation with TRAP6 or CRP-XL.

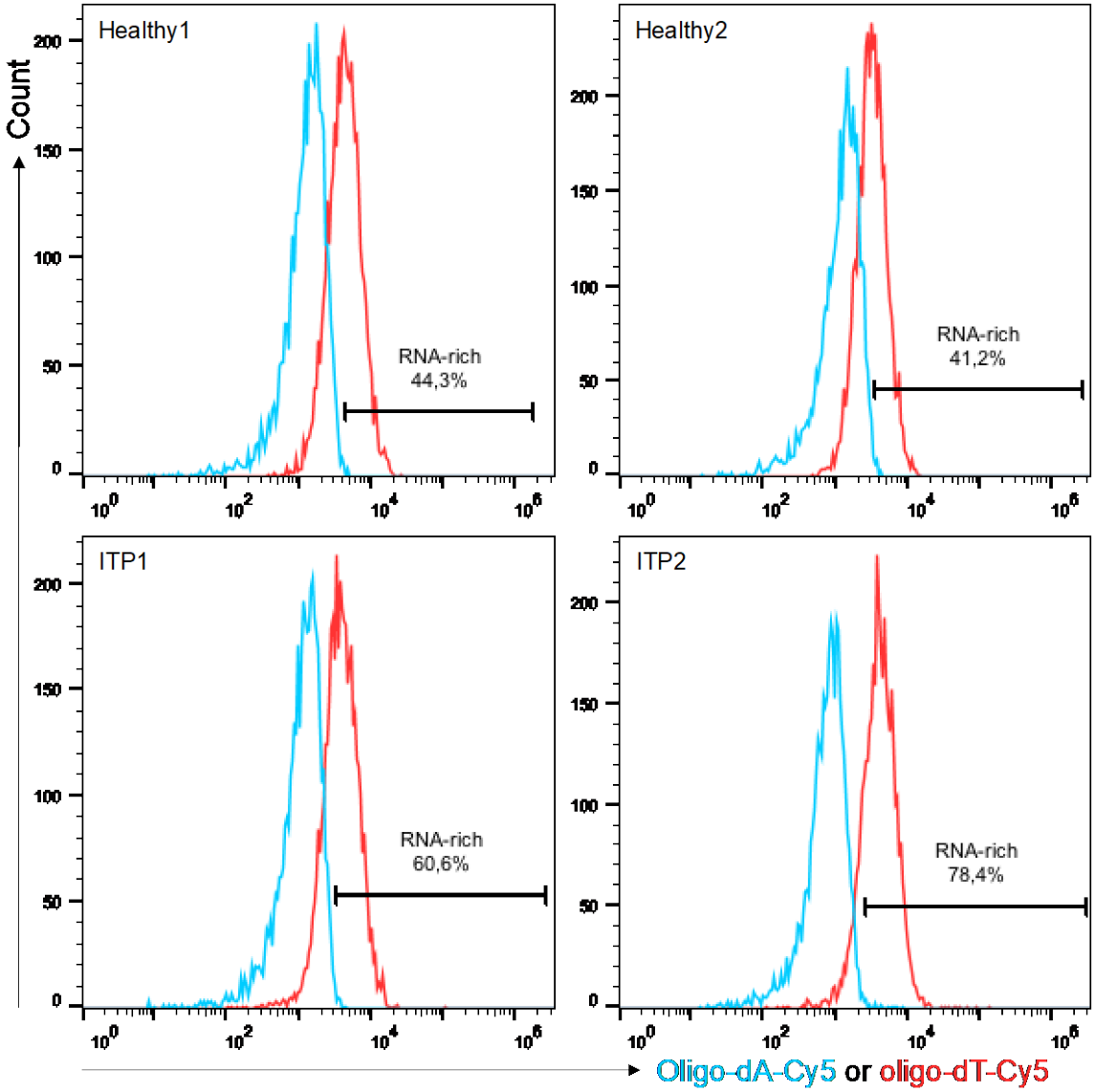

Figure S5: Determination of percentage RNA-rich platelets per healthy and ITP donor. RNA-positive platelets were determined by staining samples with either oligo-dA-Cy5 (does not bind RNA; 'isotype control') or oligo-dT-Cy5 (binds RNA specifically). This was done for each donor in quadruplo. By placing a marker at top 0,5% of oligo-dA histogram per donor, the proportion of RNA-rich platelets was determined. Shown are the representative histograms for measurements in quadruplo per donor.

References

1. De Witt SM. Multi-parameter assessment of thrombus formation on microspotted arrays of thrombogenic surfaces. Nat Prot Exchange. 2014.
2. Herfs L, Swieringa F, Jooss N, Kozlowski M, Heubel-Moenen FCJ, van Oerle R, et al. Multiparameter microfluidics assay of thrombus formation reveals increased sensitivity to contraction and antiplatelet agents at physiological temperature. Thromb Res. 2021;203:46-56.
3. van Geffen JP, Brouns SLN, Batista J, McKinney H, Kempster C, Nagy M, et al. High-throughput elucidation of thrombus formation reveals sources of platelet function variability. Haematologica. 2019;104(6):1256-1267.

4. Monaco G, Chen H, Poidinger M, Chen J, de Magalhaes JP, Larbi A. flowAI: automatic and interactive anomaly discerning tools for flow cytometry data. Bioinformatics. 2016;32(16):2473-2480.
5. Van Gassen S, Callebaut B, Van Helden MJ, Lambrecht BN, Demeester P, Dhaene T, et al. FlowSOM: Using self-organizing maps for visualization and interpretation of cytometry data. Cytometry A. 2015;87(7):636-645.
6. Veninga A, Baaten C, De Simone I, Tullemans BME, Kuijpers MJE, Heemskerk JWM, et al. Effects of Platelet Agonists and Priming on the Formation of Platelet Populations. Thromb Haemost. 2021.
7. Baaten CC, Veenstra LF, Wetzels R, van Geffen JP, Swieringa F, de Witt SM, et al. Gradual increase in thrombogenicity of juvenile platelets formed upon offset of prasugrel medication. Haematologica. 2015;100(9):1131-1138.